

# Determining paleostress orientations from faults and calcite twins: a case study near the Sainte-Victoire Range (southern France)

O. Lacombe <sup>a</sup>, J. Angelier <sup>a</sup> and P. Laurent <sup>b</sup>

<sup>a</sup> *Université P. et M. Curie, Laboratoire de Tectonique Quantitative, Tour 26-25, E1, 4 place Jussieu, 72552 Paris, Cedex 05, France*

<sup>b</sup> *Université Sciences et Techniques du Languedoc, Laboratoire Géologie Structurale, place Eugène Bataillon, 34060 Montpellier Cedex, France*

(Received October 12, 1990; revised version accepted June 14, 1991)

## ABSTRACT

Lacombe, O., Angelier, J. and Laurent, P., 1992. Determining paleostress orientations from faults and calcite twins: a case study near the Sainte-Victoire Range (southern France). *Tectonophysics*, 201: 141–156.

This paper presents the results of the analyses of striated faults and calcite twins near a highly deformed, polyphase range, the Sainte-Victoire Mountain (southern France). We thus show that combining both paleostress indicators provides a reliable way to reconstruct polyphase tectonic evolution involving homoaxial compressional stresses. From a regional point of view, the paleostress orientations have been accurately determined. These orientations correspond to three main stages of the stress field evolution since the late Cretaceous: N–S compression (late Cretaceous to late Eocene), E–W extension (Oligocene) and ENE–WSW compression (early Miocene). During the Pyrenean N–S compression, several substages of folding, strike-slip or reverse faulting have been detected. These early tectonic events account for compressional deformations older than the late Eocene major shortening of the Provence sedimentary cover.

From the methodological point of view, tectonic investigations based on both paleostress indicators (macroscopic and microscopic) were consistent and complementary. Calcite twins often allowed determination of paleostress tensors in sites where microfaults are absent for a given tectonic event. The greater sensibility of twinning to stress is related to the lower differential stress required to activate twin gliding, compared with brittle failure. Despite local stress deviations related to structural inhomogeneities, the regional stress field remains homogeneous, and provides a basis for interpreting deformation at all scales.

## Introduction

### *Previous paleostress analyses*

During the last 15 years, determinations of paleostress orientations using striated microfaults have been carried out in various geological settings. The inversion of field data in order to obtain the regional stress is usually supported by computer-based processes (Carey and Brunier, 1974; Etchecopar et al., 1981; Angelier, 1984).

It has also been shown that microscopic analysis of calcite twinning can be used to determine principal stress directions. Since the pioneering paper of Turner (1953), numerous methodologies

have been proposed (Laurent et al., 1981, 1990; Etchecopar, 1984; Dietrich and Song, 1984), and reconstructions of paleostress orientations using calcite twins have been reported (Friedman and Conger, 1964; Friedman and Stearns, 1971; Tourneret and Laurent, 1990).

Applications of both analyses of calcite twins and fault slips to natural brittle deformation have been recently carried out in the southern Rhine Graben (Larroque and Laurent, 1988), and in the Burgundy platform (Lacombe et al., 1990b). These studies have demonstrated first the regional consistency of paleostress tensors independently derived from each type of data (macroscopic and microscopic) and secondly the usefulness of ap-

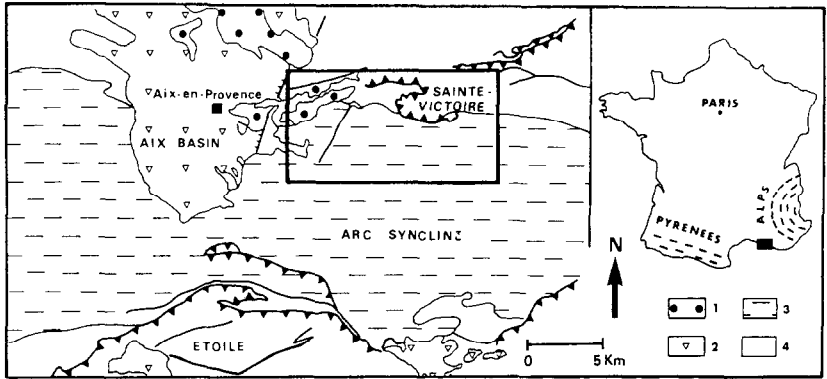


Fig. 1. Schematic sketch of southern Provence. The frame indicates the location of the area studied. 1 = Miocene; 2 = Oligocene; 3 = Late Cretaceous and Eocene; 4 = pre-Cenomanian formations.

plying both methods simultaneously in order to obtain a more accurate map of paleostress trajectories in a platform tectonics setting.

The main goals of this paper are twofold. First, we present a critical comparison of two tech-

niques of paleostress determination, based on independent paleostress indicators, striated microfaults and calcite twins. Second, we propose that it is useful to combine both these techniques, especially to reconstruct polyphase tectonic evo-

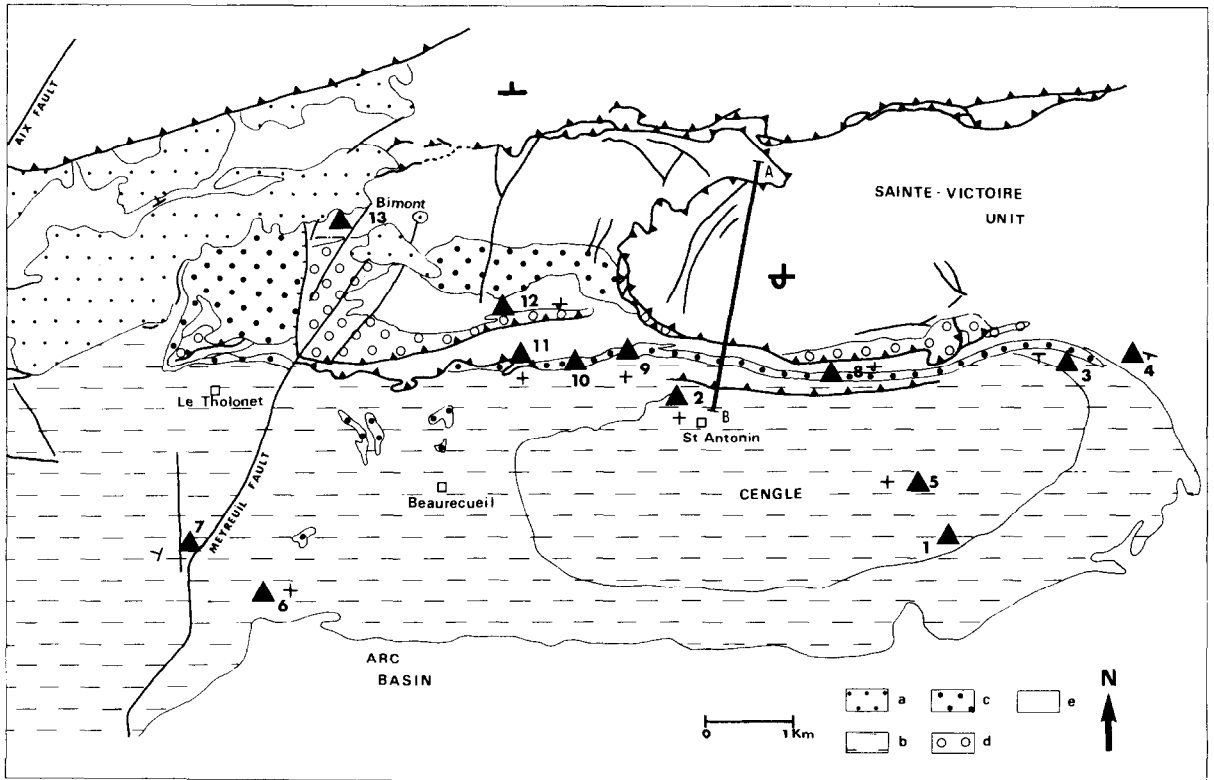


Fig. 2. Schematic structural map of the area studied. *a* = Miocene; *b*, *c* = Eocene (*c* = Dano-Montian breccia); *d*, *e* = pre-Cenozoic formations (*d* = late Campanian breccia). Large black triangles indicate sites of data collection (1-13). A-B = cross-section shown in Fig. 3. Stratigraphic and tectonic contacts after Catzigras et al. (1969).

lution involving homoaxial compressional stresses. For this aim, the Sainte-Victoire Range (southern France) provides a good regional basis for a case study (Fig. 1).

#### *Choice of the study area*

The investigated area is the Sainte-Victoire Mountain, a E–W-trending fold-and-thrust range (Figs. 1 and 2). This range is commonly interpreted as being due to the thrust development of a former fold. The overturned southern flank of this fold was secondarily thrust southwards on to the northern margin of the Arc basin (Durand and Tempier, 1962; Corroy et al., 1964; Figs. 2 and 3). Regional-scale structures indicate that the tectonic evolution of the range has involved successive episodes of deformation since the late Cretaceous. West of the range, the Aix-en-Provence faulted basin developed during Oligocene time. The Oligocene formations are downfaulted beside, and unconformably overlie, the compressional features of the range (Fig. 1).

This structural setting (Fig. 2) has been chosen for several reasons. First, outcropping formations along the Sainte-Victoire Range include syntectonic deposits, which may indicate the timing of successive tectonic events (Fig. 3). Second, microtectonic evidence for polyphase deformation was found in several sites (e.g., successive striations on faults or cross-cutting relationships between faults). Note also that the association of folds and thrusts with complex patterns of minor faults and

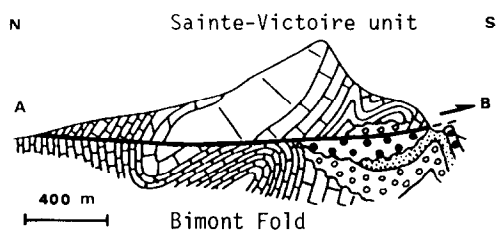


Fig. 3. Geological cross-section through the Sainte-Victoire structure (from Tempier and Durand, 1981). Location as A–B on Fig. 2. Lithology: brick pattern = Jurassic limestones; simple lines = early Cretaceous formations; small open circles = late Campanian breccia; dots = Maestrichtian formations; heavy black dots = Dano-Montian breccia. Note the unconformable attitude of the two breccia formations with regard to the Bimont fold.

tension gashes allows reconstruction of the relative chronology of faulting events, primarily on the basis of fault attitudes with respect to stratal tilting. Third, the presence near the thrust of early Tertiary subhorizontal limestones makes microscopic analysis of the crystalline deformation possible. In these limestones, coarse-grained vacuols, fossil infills or sparitic cement display clear xenomorphic large calcite crystals, which are suitable for the study of calcite twinning.

#### **Methods for reconstructing paleostress orientations**

##### *Determination of paleostress orientations using striated faults*

Following the inverse method proposed first by Carey and Brunier (1974), populations of striated faults have been interpreted in terms of stress tensor determinations, assuming a relationship between the actual observed slickenside lineation and the direction of the resolved shear stress on the fault plane (Bott, 1959). The obtained stress tensor characterizes the stress regime according to which slip on the fault plane occurred. It accounts for four independent parameters among the six of the complete stress tensor. These four parameters are the orientations of the three principal stresses  $\sigma_1$ ,  $\sigma_2$  and  $\sigma_3$ , as well as the ratio  $\Phi = (\sigma_2 - \sigma_3)/(\sigma_1 - \sigma_3)$  between their magnitudes. Herein,  $\sigma_1$  is the greatest principal compressive stress,  $\sigma_2$  is the intermediate principal stress and  $\sigma_3$  is the least compressive stress (compressions counted as positive). The calculation of regional stress directions through a computer-based inversion of field data, as well as the procedure for separating successive stress tensors and related subsets of fault slip data, have already been presented and discussed in detail (Angelier, 1984).

##### *Determination of paleostress orientations using calcite twins*

At the pressures and temperatures likely to be found in sedimentary basins, calcite deforms primarily by twin gliding on  $e$  planes [10 $\bar{1}$ 2]. This

mechanical twinning in calcite crystals results in a change in the form of the crystal by an approximation to simple shear in a particular sense and direction on crystallographic  $e$  planes (Turner et al., 1954).

To occur, twin gliding in calcite requires a resolved shear stress (i.e. the component of stress along the twinning direction) that exceeds a critical value  $\tau_a$  (the yield stress value for twinning). According to experiments by Turner et al. (1954), this critical value averages 10 MPa. The yield stress value for twinning is independent of temperature, confining pressure and is only slightly dependent upon deformation rate (Friedman and Heard, 1974; Tullis, 1980), but Rowe and Rutter (1990) show that it is grain-size dependent. However, as the size of the crystals measured in our samples is homogeneous (200–300  $\mu\text{m}$ ), the use of inverse methods is theoretically justified (Rutter, pers. commun., 1990). Ninety randomly oriented crystals were examined in each sample using a universal stage. In each crystal, the spatial orientation of the three potential twin planes was defined, and the twinned or untwinned character was optically checked.

The calculation of the stress tensor which accounts for the largest number of twins is made through the computer-based inversion of calcite twin data (Laurent et al., 1981, 1990; Etchecopar, 1984). In the present paper, Etchecopar's inverse method, which has proved suitable for the study of samples concerned with polyphase tectonics (Larroque and Laurent, 1988; Lacombe et al., 1990b), has been used. Mathematical aspects, separation of different stress tensors and related data subsets when deformation is polyphase and limits of the method were discussed by Etchecopar (1984), Tournieret and Laurent (1990) and Lacombe et al. (1990b). This method provides direct access to the orientations of the three principal stresses,  $\sigma_1$ ,  $\sigma_2$  and  $\sigma_3$ , and to the ellipsoid shape ratio  $\Phi$  defined above.

#### Results: fault patterns and paleostress orientations near the Sainte-Victoire Range

Three main regional paleostress systems have been defined in the area of Fig. 2, based on

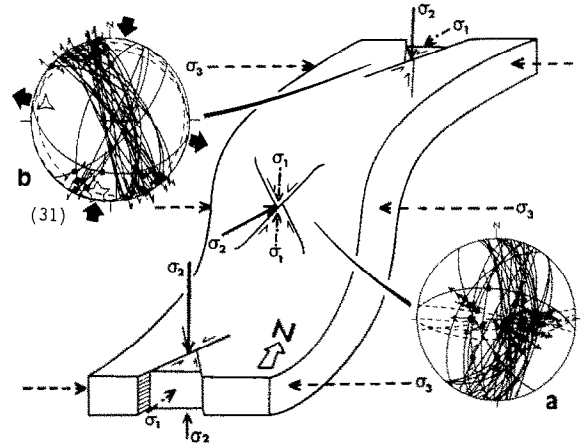


Fig. 4. Schematic block diagram which illustrates interactions between folding and strike-slip faulting. Data are plotted in lower-hemisphere, equal-area projection with the plane of the projection horizontal and the north as indicated. Faults are shown as thin curves and slickenside lineations as dots with double arrows (left- or right-lateral) or simple ones (centrifugal = normal, centripetal = reverse). Paleostress directions as empty stars with five branches = maximal compressive stress  $\sigma_1$ ; four branches = middle stress  $\sigma_2$ ; three branches = minimal stress  $\sigma_3$ . Directions of extension or compression shown by large black arrows. The bedding plane is represented as a dashed line. Diagram (a) represents present fault attitude (normal fault pattern) on vertical state of site 13. Diagram (b) illustrates backtilted fault attitude and the corresponding principal stress directions. The number in parentheses indicates how many fault-slip data are plotted on the diagram.

macroscopic (faults) and microscopic (twins) analyses. In this section, we briefly present the main results (Figs. 4–8). The problem of the earliest stages of faulting, which predate most of the folding and thus require particular analysis (such as in Fig. 4), will be discussed in the subsequent section.

#### *N–S compression*

Regardless of various stratal attitudes (sub-horizontal or dipping), layers at sites 2, 6, 9, 10, 11 and 12 (Fig. 2) are cut by subvertical strike-slip faults with consistent orientations. Subvertical tension gashes striking N–S (Fig. 5) are associated with these fault patterns. The azimuths of left-lateral strike-slip faults range from 005° to 040° (i.e. N5°E to N40°E), whereas those of right-lateral strike-slip faults range from 130° to 160° (Fig. 5). The computed stress tensors show

horizontal  $\sigma_1$  axes trending around N-S, and horizontal  $\sigma_3$  axes trending E-W (Table 1). Calcite twins also record this stress regime in the Cenozoic limestones (Table 2): computed  $\sigma_1$  axes are subhorizontal and range from  $350^\circ$  (site 2) to  $201^\circ$  (site 1).

Numerous minor reverse faults trending  $060^\circ$  to  $100^\circ$  have also been observed (Fig. 6). These reverse faults affect tilted layers as well as subhorizontal ones. The computed  $\sigma_1$  axes are approximately horizontal, with fairly homogeneous trends from  $170^\circ$  to  $020^\circ$  (Fig. 6 and Table 1). The stress tensor determined from calcite twins at site 6 shows an horizontal  $\sigma_1$  axis trending  $358^\circ$ . This N-S direction of compression provided by both indicators is in agreement with N-S average trends of subhorizontal stylolites.

### *E-W extension*

At site 11, normal faults in subhorizontal layers allowed reliable calculation of a stress tensor with a vertical  $\sigma_1$  axis. The  $\sigma_3$  axis is horizontal and trends approximately E-W (Fig. 7). At sites 1, 2, 7 and 9, the trends of  $\sigma_3$  axes provided by calcite twin analysis range from  $069^\circ$  (site 1) to  $094^\circ$  (site 9) (Fig. 7 and Table 2). Note that no normal fault was found at these stations.

### *WSW-ENE to NW-SE compressions*

Despite the absence of related macroscopic features, two main sets of  $\sigma_1$  orientations have been characterized at sites 1, 2, 6, 7 and 9 from calcite twins. As Fig. 8 and Table 2 show, the  $\sigma_1$

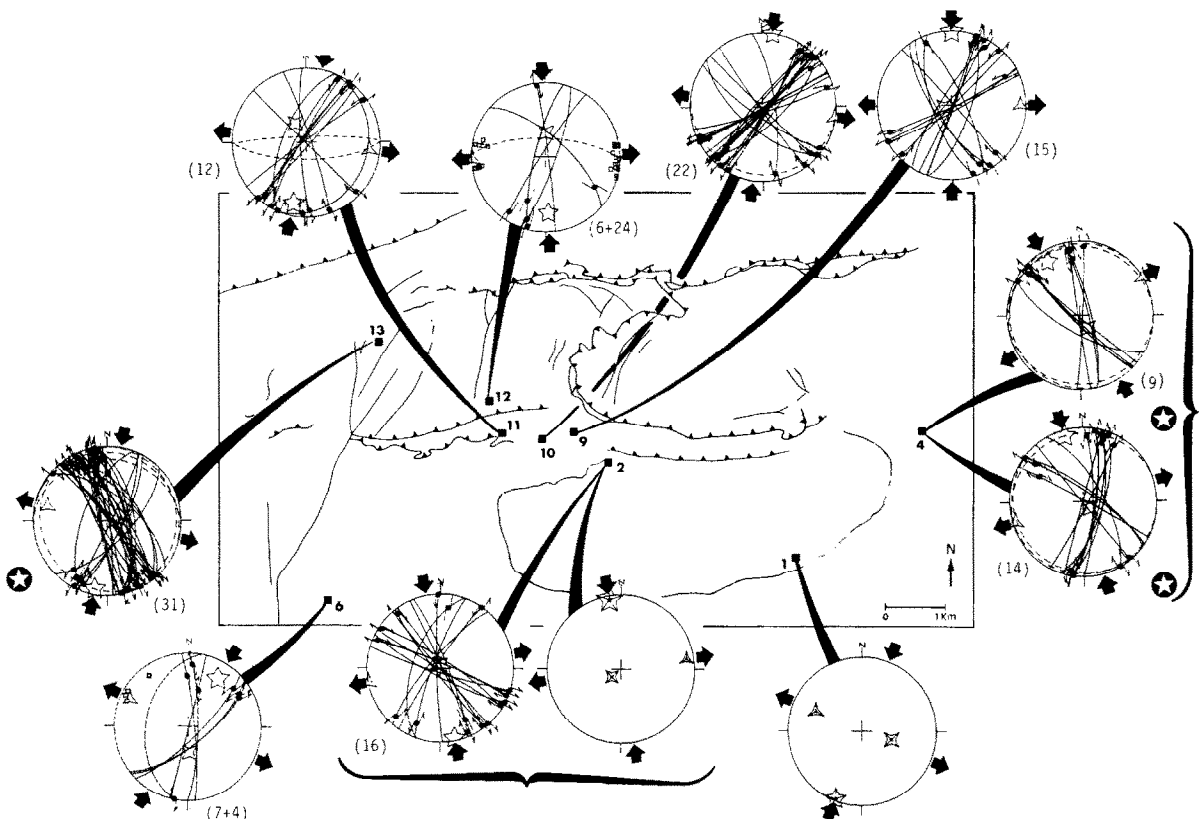


Fig. 5. N-S compression (strike-slip fault regime) inferred from striated microfaults and calcite twins. Data are plotted in lower-hemisphere, equal-area projection with the plane of the projection horizontal and the north as indicated. For fault slip data, same key as in Fig. 4. Calcite twin data: paleostress directions shown as ornate stars, with three, four or five branches (as for fault-slip analysis). For sites where faults have been tilted secondarily, the diagrams with stars illustrate backtilted fault attitude and the corresponding stress tensor. Poles of tension gashes shown as empty squares. As in Fig. 4, the number in parentheses indicates how many fault-slip data (plus number of poles of tension gashes where present) are plotted on each diagram (see also Table 1).

axes are horizontal. Their azimuths range either from 042° to 070° or from 094° to 120° (Fig. 8).  $\sigma_3$  axes are horizontal in the first case (sites 2, 6 and 7) and vertical in the second one (sites 1, 2, 7 and 9), indicating a predominantly strike-slip or pure compressional regime respectively. At some sites, both stress tensors were reconstructed (sites 2 and 7, Fig. 8 and Table 2).

### Interpretation of results: the paleostress evolution in the Sainte-Victoire area

The identification of three major paleostress systems in the area studied shows that its tectonic

evolution is polyphase, in agreement with the results of previous structural studies. As a result, it is necessary to examine the succession of events in more detail in order to reconstruct the tectonic evolution of this region.

### Late Cretaceous to Late Eocene N-S compression

At most sites, the subvertical strike-slip faults and the associated tension gashes, as well as reverse faults, affect rock formations regardless of their various stratal attitudes. Consequently, they should be related to post-folding faulting.

Consideration of geometrical relationships be-

TABLE 1  
Paleostress tensors computed from fault-slip analysis

SITES	$\sigma_1$	$\sigma_2$	$\sigma_3$	$\Phi$	N	ANG
(1)	002-03	092-01	207-87	0.56	37	9 (III)
(2)	169-04	354-86	259-00	0.38	16	9 (IV)
(3)	158-14	250-05	000-75	0.66	7	7 (III)
(4)	179-10	271-10	047-76	0.60	28	12 (III)
	329-16	150-74	059-00	0.47	9	5 (II)
(5)	345-09	135-80	254-05	0.36	14	10 (II)
	178-12	269-04	018-78	0.40	6	7 (III)
(6)	014-02	284-07	121-82	0.59	40	12 (III)
	032-24	177-61	295-15	0.29	7	9 (IV)
(7)	012-05	281-10	130-79	0.47	21	11 (III)
(8)	174-13	083-05	333-76	0.74	24	12 (III)
(9)	185-00	095-06	278-84	0.54	11	13 (III)
	001-02	258-82	091-08	0.32	15	10 (IV)
(10)	352-01	262-10	087-80	0.69	8	7 (III)
	008-01	212-89	098-00	0.45	22	7 (IV)
(11)	207-06	116-09	328-79	0.40	10	6 (III)
	351-18	088-20	222-62	0.29	15	8 (III)
	192-18	330-66	097-15	0.40	12	10 (IV)
(12)	016-75	189-15	279-02	0.41	6	14
	178-26	001-64	268-01	0.49	6	15 (IV)
(13)	191-08	077-70	284-19	0.40	31	12 (I)

For sites where faults have been tilted secondarily, these characteristics are related to back-tilted fault attitude. Stress axes: trend and plunge in degrees.  $\Phi = (\sigma_2 - \sigma_3) / (\sigma_1 - \sigma_3)$ , defined in text.  $N$  = number of faults consistent with the tensor;  $ANG$  = average angle between computed shear stress and observed slickenside lineation, (in degrees). For stress tensors related to the N-S compression, the roman numerals in parentheses indicate the probable corresponding tectonic event (see text and Table 3).

tween fault patterns and tilted strata also enabled us to distinguish pre-folding paleostress systems. The distinction between pre- and post-folding episodes is important in establishing a chronological succession of faulting events, because the timing of fold development is known from syntectonic deposits (Fig. 3). As an example, at site 13 (Fig. 2), the subvertical reverse flank of the Bimont fold (a fold of Jurassic limestones and dolomites with an E-W-trending axis) is affected by N-S-trending faults. In their present position, these faults are normal dip-slip (Fig. 4). The tensor computed from these normal faults corresponds to an horizontal  $\sigma_3$  axis, parallel to the strike of beds in the flank of the anticline and to the fold axis. The  $\sigma_1$  axis is parallel to the bedding and to the dip direction (Fig. 4). With the reasonable assumptions that folding was cylindrical with an horizontal axis, and that bedding was approximately horizontal when strike-slip faulting

occurred, these geometrical relationships indicate that the fault pattern observed at site 13 results from fold-induced tilting of early strike-slip faults. The N-S direction of the backtilted  $\sigma_1$  axis is perpendicular to the fold axis (Fig. 4). This pattern of principal stresses and genetically related strike-slip shear fractures or faults is identical to that found on folds worldwide, and is referred to as shear fracture assemblage (Friedman and Stearns, 1971). We conclude that faulting and folding probably correspond to a single compressional event. At site 4 (Fig. 2), a similar geometrical analysis also suggests that the present pattern of reverse and normal faults results from the tilt of an early system of conjugate strike-slip faults. The backtilted  $\sigma_1$  axis is compatible with N-S compression (Fig. 5).

In addition to the general identification of structures related to the N-S compression, the analysis of faulting-folding relationships thus

TABLE 2

Paleostress tensors computed from calcite twin analysis

SITES	$\sigma_1$	$\sigma_2$	$\sigma_3$	$\Phi$	N1	N2	N3
(1)	290-19	039-43	182-41	0.47	205	29	61
	201-03	106-56	293-33	0.40	205	29	43 (IV)
	062-71	158-02	249-19	0.54	205	29	40
(2)	350-06	231-77	081-11	0.15	219	36	87 (IV)
	274-01	184-08	010-82	0.27	219	36	39
	071-64	167-03	258-26	0.41	219	36	27
(6)	222-18	038-72	132-01	0.50	219	36	31
	233-80	137-01	047-10	0.63	203	41	81
	358-04	268-06	121-83	0.26	203	41	36 (III)
(7)	068-28	258-61	161-04	0.40	203	41	43
	301-01	031-02	192-88	0.18	221	30	88
	240-19	098-67	335-13	0.56	221	30	66
(9)	002-53	159-35	257-11	0.53	221	30	40
	289-18	191-23	053-61	0.79	231	31	80
	146-59	013-22	274-20	0.43	231	31	37

Key for stress axes and  $\Phi$  ratio as in Table 1.  $N_1$  = total number of twinned planes measured;  $N_2$  = total number of untwinned planes measured;  $N_3$  = number of twinned planes compatible with each tensor solution. Roman numerals in parentheses used as in Table 1.

leads us to distinguish pre-tilt and post-tilt fault systems. This allows us to recognize second-order substages of deformation during the N-S compression (Figs 5 and 6). Stratigraphic and structural criteria observable in the field were used to establish the chronology of these substages. These criteria are as follows.

(1) Early strike-slip faults developed first in the subhorizontal late Jurassic formations of site 13. These faults have been secondarily tilted during folding. The existence of two steps of folding is ascertained by syntectonic breccia deposits, late Campanian and Dano-Montian in age, which rest unconformably on the flank of the Bimont fold (Corroy et al., 1964; Fig. 3). We conclude that strike-slip faulting occurred before the late Campanian.

(2) The formations of the Maestrichtian display clear time relationships between strike-slip faulting, folding and reverse faulting at site 4. Early strike-slip faults have been tilted when folding occurred. Late reverse faults cross-cut tilted strata.

(3) The youngest formations affected by reverse faults are Lutetian in age (top of the Cenge plateau, site 5). As these reverse faults do not apparently affect Oligocene formations, it is likely that reverse faulting occurred during the late Eocene.

(4) Finally, late strike-slip faults clearly intersect and offset reverse faults at site 7.

On the basis of these combined stratigraphic and paleostress analyses, we finally reconstructed the succession of faulting events associated with

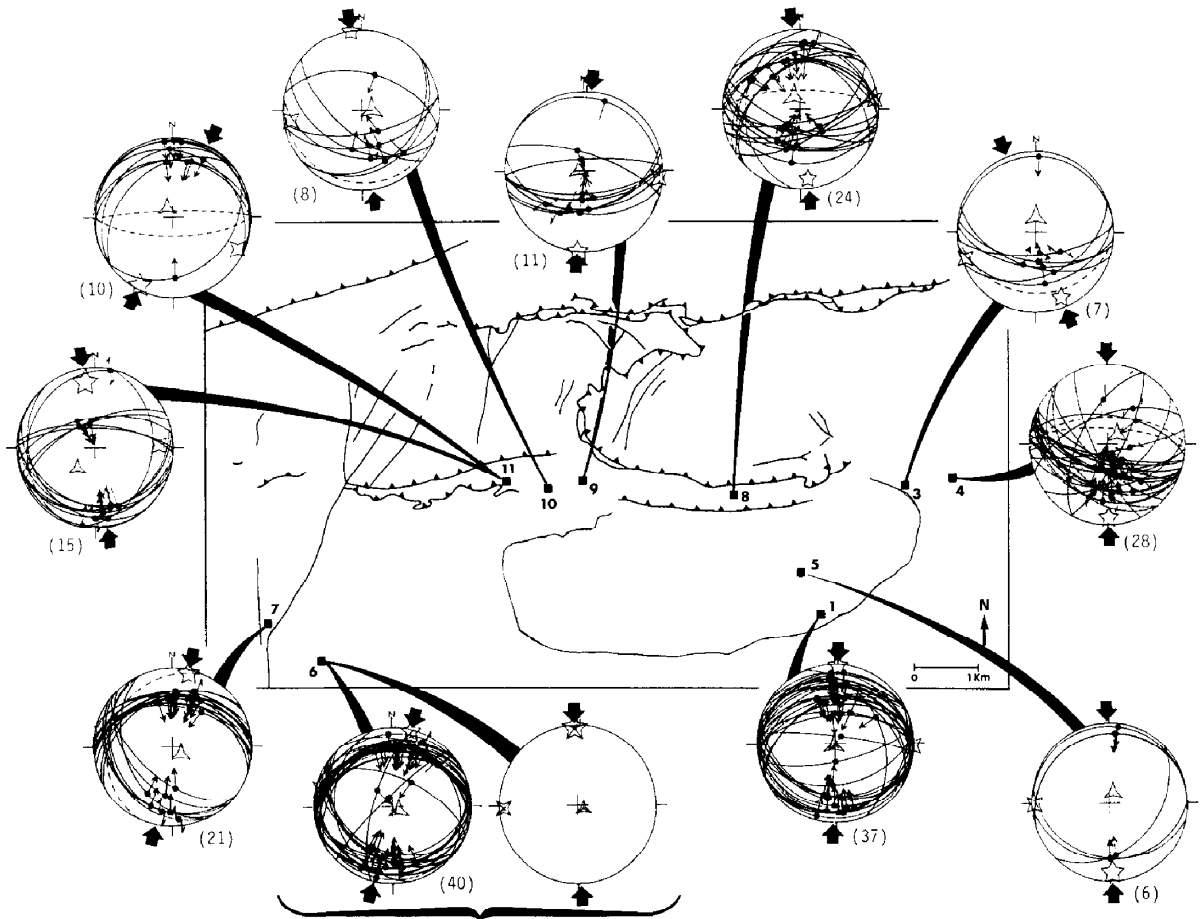


Fig. 6. N-S compression (reverse fault regime). Key as Fig. 5.

N-S compression (Table 3). The first strike-slip regime occurred before the late Campanian (event I). This was followed by the first step of folding, with deposition of syntectonic late Campanian breccia. A second strike-slip fault regime developed during the late Maestrichtian (event II). This was followed by the second and major step of regional folding, with deposition of the syntectonic Dano-Montian breccia. This compression continued with thrust emplacement associated with reverse faulting during the late Eocene paroxysmal tectonism (event III). Finally, a last strike-slip regime took place (event IV), just before Oligocene extension.

#### *Oligocene E-W extension*

The approximately E-W orientations of  $\sigma_3$  axes derived from faults and calcite twins (Fig. 7) are in good agreement with the directions of

extension reconstructed in the Arc basin by Gonzales (1989), or in Oligocene formations north of Aix-en-Provence by Hippolyte (pers. comm., 1990). Furthermore, a 030°-trending segment of the Aix fault which affects the Oligocene formations along the Aix basin was active during the Oligocene infilling of the basin (Nury, 1980). These observations suggest that the E-W extensional paleostress regime is related to the major extension responsible for the development of the Aix-en-Provence basin during the Oligocene.

#### *Miocene WSW-ENE to NW-SE compressions*

The 070° orientations of  $\sigma_1$  axes deduced from calcite twins (Fig. 8) are quite similar to the direction of compression found by Gaviglio and Gonzales (1987) in the Arc basin using striated microfaults. Although no striated fault marks this compression in the area studied herein, calcite

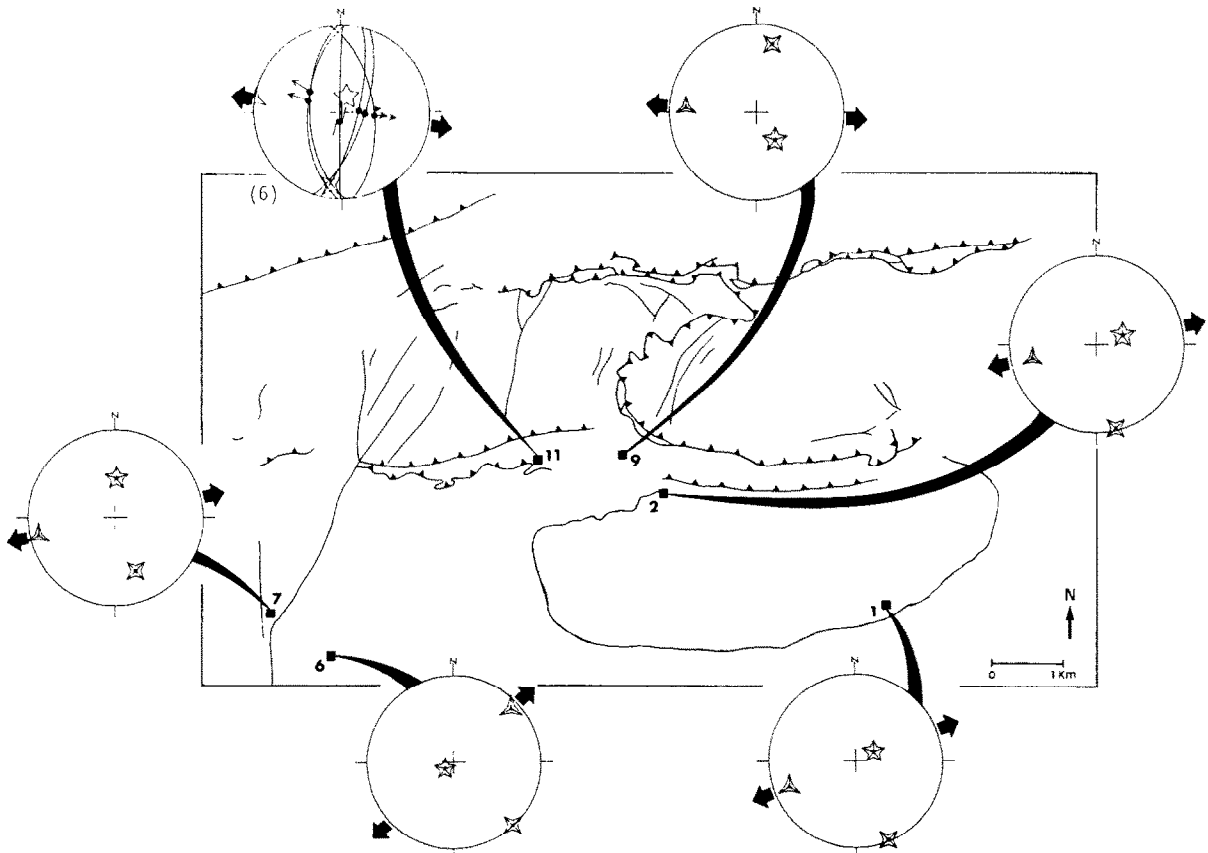


Fig. 7. E-W extension. Key as Fig. 5.

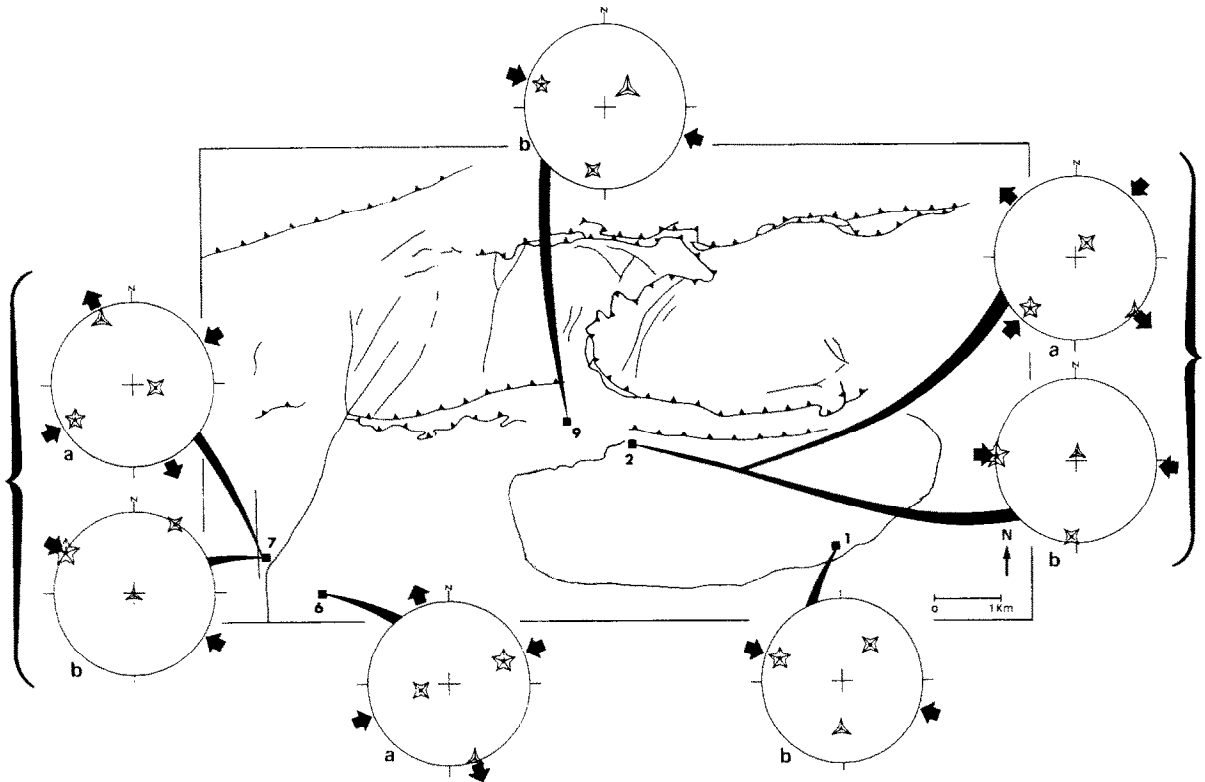


Fig. 8. ENE-WSW to NW-SE compressions. Key as Fig. 5.

twins recorded this  $070^\circ$  compressional strike-slip regime at sites 2, 6 and 7 (Fig. 8 and Table 2). All stress tensors with azimuths of  $\sigma_1$  ranging from

$042^\circ$  to  $070^\circ$  may be related to a single compressional event. This event probably occurred after the Oligocene and before the Tortonian, because

TABLE 3

Synthetic tectonic evolution of the area studied

	Tectonics	Stresses
Post-Tortonian	Reverse and strike-slip faults	N-S to N20° "alpine" compression
Early Miocene	Strike-slip faults	N70° early "alpine" compression
Oligocene	Normal faults	E-W extension
Eocene	Strike-slip faults (IV)	
	Reverse faults (III)	
	Major tangential episode	
Paleocene	Major episode of folding. Dano-Montian breccia	N-S "pyrenean" compression
	Strike-slip faults (II)	
Late Cretaceous	Early episode of folding. Late Campanian breccia	
	Strike-slip faults (I)	

the Oligocene formations of Aix-en-Provence are affected by this compression (Hippolyte, pers. commun., 1990) whereas Tortonian formations are not (Gaviglio and Gonzales, 1987). This event, probably early Miocene in age, may correspond to Alpine compression.

The  $\sigma_1$  orientations ranging from  $094^\circ$  to  $120^\circ$  (Fig. 7) are surprising, because no paleocompression of this direction has been mentioned in the literature in the area of interest. Late Alpine compression was N–S in Provence and the southwestern external Alps (Bergerat, 1985). However, as consistent  $\sigma_1$  orientations were systematically and independently recognized at sites 1, 2, 7 and 9 (Fig. 8), we must consider these results to be geologically significant. Rather than defining a new tectonic phase, which is not supported by other regional data, we suspect that these orientations correspond to strong stress deviations of the  $070^\circ$   $\sigma_1$  trajectories. These deviations occur in the vicinity of a major discontinuity, the Aix-en-Provence/Meyreuil fault system. Such stress perturbations may be interpreted either as a deflection of stress before fault movement (Arthaud and Choukroune, 1972; Trémolières, 1981), or as a dragging effect due to shear movement in the vicinity of the fault (Letouzey, 1986). The magnitude of the deviated stress was probably not large enough to cause failure; however, it reached the yield stress value for calcite twinning (see next section). This explains why these stress orientations were not recorded by faulting and were not described before.

### Comparison of macroscopic and microscopic paleostress analyses

#### *Errors and individual uncertainties inherent in the methods*

Detailed discussions about the inversion of fault slip and calcite twin data were published previously (see Angelier, 1984, 1990 for striated faults; Laurent, 1984; Laurent et al., 1990 for calcite twins). However, estimates of methodological uncertainties inherent in both techniques of paleostress determination are needed in order to allow efficient comparisons.

For calcite twins, the extent of uncertainties in inversion process was empirically estimated in Laurent et al. (1990). For a given monophase sample, the uncertainties in the paleostress orientations derived using Etchecopar's method and the method proposed by Laurent et al. (1990) are less than  $5^\circ$ . The presence of stylolites in the same thin section where measurements were carried out confirm the accuracy of the stress orientations determined. This study indicates that the largest source of uncertainties for usual numbers of twin data (30–120) is not the inversion process, but the errors in thin section orientation and U-stage measurements. The most pessimistic estimation involves a maximum error of about  $10$ – $15^\circ$ . Usually, stress orientations are defined with uncertainties of about  $5$ – $10^\circ$ . As a consequence, the paleostress tensors presented herein are reliable solutions (Table 2). Furthermore, experiments made with deletions or additions of few twin data indicated that the solutions are computationally stable within an accuracy of  $5$ – $10^\circ$ . In contrast, determination of the  $\Phi$  ratio is not well constrained. It is highly dependent on the number of twinned planes used for its calculation, and uncertainties may be as large as  $\pm 0.3$ .

For striated microfaults, theoretical and practical estimates of uncertainties have been discussed in Angelier et al. (1982). The major source of errors lies in the data acquisition, provided that the number of fault slip data is large enough (usually, 15–200), and that there is a large variety of fault attitudes. In this case, no significant source of uncertainties results from the inversion process itself. Errors inherent in data collection cause angular uncertainties in stress axis determinations, of about  $5$ – $15^\circ$ . As for calcite twins, uncertainties on determination of  $\Phi$  ratios are much larger (i.e.  $\pm 0.2$ ).

#### *Polyphase faulting and twinning*

The polyphase character of the brittle deformation was easily recognized at the macroscopic scale (regional-scale folds and thrusts, and successive fault slips). It was also expected at the microscopic scale. Our results supported this expectation: polyphase twinning was clearly de-

tected. Each of the successive stress tensors derived from calcite twins from a given sample accounts for only 20–30% of the twinned lamellae measured. The number of twinned planes consistent with each computed tensor is given in the last column ( $N_3$ ) in Table 2. For instance, the tensors successively determined in site 1 account respectively for 30% (61/205), 21% (43/205) and 20% (40/205) of the total set of twinned planes measured (205). Thus, twinning in our samples always resulted from two or more superimposed tectonic paleostresses. The remaining 29% (60/205) of twinned planes are incompatible with these three main tensors, and may simply correspond to primary twins (syndimentary or syndiagenetic twins).

#### *Consistency of paleostress orientations derived from fault slips and calcite twins*

Following the previous works of Larroque and Laurent (1988) and Lacombe et al. (1990b), calcite twin and fault slip analyses were expected to provide regionally consistent results in terms of paleostress orientations. Effectively, our study demonstrates that taking into account uncertainties inherent in the methods, both paleostress indicators yield very similar paleostress orientations at the regional scale, despite the complexity of the structural setting. Principal stress directions inferred from crystallographic data were found to be similar to those reconstructed from striated faults (Figs. 5–8, Tables 1 and 2). These stress directions are also consistent with additional tectonic data (fold axes, stylolites). This provides further evidence for the consistency of regional paleostress reconstructions, and for the suitability of these paleostress reconstructions to account for the regional tectonic evolution.

#### *Sensibility of indicators to paleostress*

Presumably, according to the low yield stress value for twinning in calcite (approximately 10 MPa), calcite twinning requires a lower differential stress to occur, compared with brittle failure or frictional sliding on previously formed planes. Effectively, at most sites, stress tensors corre-

sponding to E–W extension and 070° compression could be derived only from calcite twins (Figs. 7 and 8). For these two tectonic phases, it is thus likely that principal stress values have not been large enough to induce macroscopic rock failure. Moreover, as the yield stress value for twinning is independent of confining pressure, an increase in confining pressure might also cause twinning to occur, while faulting did not. We conclude that twinning is a more sensitive paleostress indicator than microfaulting, and thus records weak but significant paleostress regimes. We point out that accurate paleostress analyses should combine both paleostress indicators, macroscopic and microscopic, in order (1) to check for consistency and (2) to significantly increase the regional density of paleostress determination network.

#### **Local stress perturbations, regional paleostress and scale changes**

Local conditions may introduce some discrepancies in the stress tensors derived. These discrepancies may concern the stress orientations as well as the ellipsoid shape ratio  $\Phi$ , but the influence of these local effects on reconstructions of regional paleostress orientations remains small. It is important to point out again that these discrepancies cannot be accounted for by technical uncertainties, which are much smaller.

#### *Variations in stress orientations*

Taking into account the usual uncertainties of about 5–10° in paleostress orientations, deviations larger than 15–20° from the N–S direction should be explained in terms of local stress perturbations due to inhomogeneities in rocks. Such rotations of principal stress are easy to detect provided that the observation network is dense enough. For instance, they may occur in the vicinity of reactivated strike-slip faults oblique to the main stress axes. Such deviations have been already discussed on the basis of finite element analyses (Xiaohan, 1983), and compared with actual fault patterns (Taha, 1986; Lacombe et al., 1990a). This case is illustrated in Fig. 9, where  $\sigma_1$

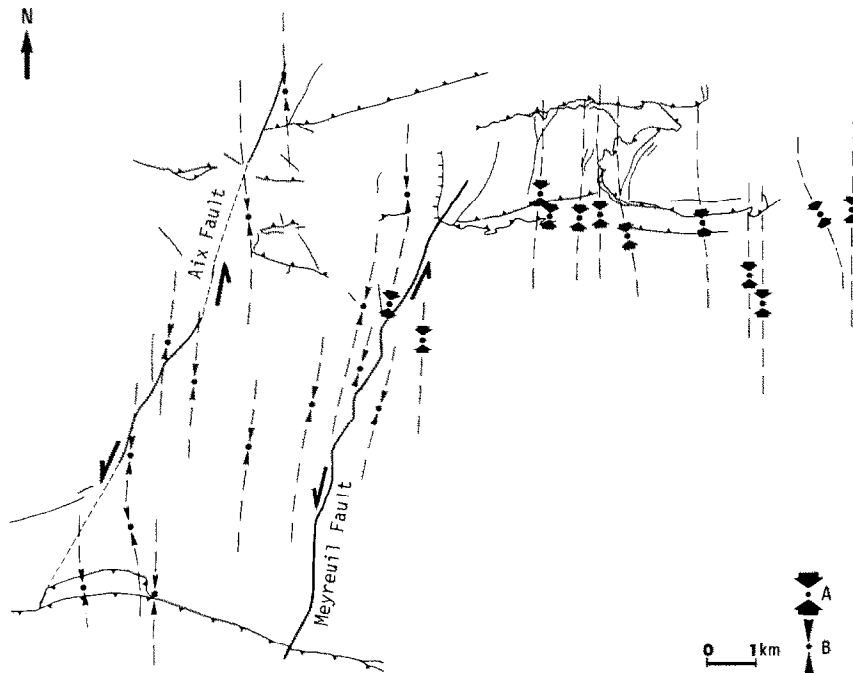


Fig. 9. Paleostress trajectories reconstructed for the Eocene episode of N-S compression. (A) Directions of  $\sigma_1$  reconstructed in the present work. (B) Directions of  $\sigma_1$  reconstructed by Gonzales (1989). Note the deviation of stress trajectories close to the Aix-en-Provence/Meyreuil fault system.

axes re-orient and become subparallel to the Aix/Meyreuil fault system.

#### *Variations in $\Phi$ ratios*

The variability in the  $\Phi$  ratios derived may be also ascribed to local stress perturbations, without significant variation in paleostress orientations (Tables 1 and 2). Theoretically, the notion of a stress tensor involves a point source character. Geologists using fault analysis commonly assume that the stress ellipsoid shape ratio is constant in the rock volume considered ( $10^3$  to  $10^6$  m<sup>3</sup>), the usual volume of a microtectonic station. In contrast, calcite twin analysis allows determination of paleostress tensors in very small rock volumes ( $10^{-3}$  m<sup>3</sup>). Attention should be paid to this change in scale. Experiments (Barquins et al., 1989a, b; Petit and Barquins, 1990) have shown that within a small pre-fractured sample of homogeneous rock submitted to uniaxial stress, the ratio  $\Phi$  may vary around the pre-existing defect. As a consequence, stress perturbations added to methodological uncertainties explain why variable

values of ratio  $\Phi$  are obtained in a given site for a given tectonic event, on the basis of analyses of fault slips and calcite twins in a complex structural setting. The differences in the scales considered (rock mass and sample, respectively) partly account for such apparent discrepancies. Usually, the range of misfits in ratio  $\Phi$  determinations remains smaller than  $\pm 0.4$ . Fortunately, this variability does not reduce the usefulness of paleostress indicators in terms of orientations, because it has very little influence on the reconstructed paleostress directions, as additional runs of inversion methods have shown (see also Tables 1 and 2).

Consequently, as paleostress analyses usually rely upon a large number of measurements and derived stress tensors, stress perturbations detected appear to be only local effects within a very homogeneous paleostress field (Fig. 9). The regional stress history deduced from the paleostress indicators must thus be considered to be reliable. In a complex tectonic setting such as for the Sainte-Victoire Range (Figs. 2 and 3), paleostress orientations inferred from both pa-

leostress indicators are remarkably homogeneous and consistent in the whole area (Figs. 5 and 6). All the main structures, from the regional scale (folds, thrusts and wrench faults), to the micro-tectonic scale (microfaulting and crystalline deformation) are accounted for by a single homogeneous paleostress regime with a general  $\sigma_1$  axis that is horizontal and trending N–S (Fig. 9).

### **Paleostress reconstructions and regional tectonic evolution**

The tectonic emplacement of the Sainte-Victoire thrust (Figs 2 and 3), as well as most of the brittle deformation that we have observed, should be interpreted within the framework of the shortening of the Provençal sedimentary cover at the time of the Iberia–Eurasia collision. This N–S compression is a major characteristic of the Pyrenean foreland (Mattauer and Mercier, 1980), and more generally of the Western European platform (Bergerat, 1985).

At the scale of the area studied (Figs. 2 and 9), the paleostress regime (horizontal N–S compression), has prevailed from the late Cretaceous to the late Eocene, accounts for the development of regional-scale structures, which accommodate the displacement and the shortening of the sedimentary cover. A more accurate paleostress analysis has enabled us to detect and separate second-order tectonic events, which should be considered as successive substages of the continuous N–S compressional phase, occurring from the late Cretaceous to the late Eocene. Most of the tectonic shortening was accomplished during the late Eocene major event (Tempier, 1987). Older tectonic events (late Cretaceous and Paleocene in age) have resulted in smaller displacements. However, their role was essential, because discontinuities and zones of weakness were thus created in the cover and became available for reactivation.

The extensional paleostress regime with a  $\sigma_3$  axis oriented E–W could be detected far away from the major basin faults using calcite twins (Fig. 7). This stress regime accounts for the development of the Aix-en-Provence Oligocene basin. More generally, it may be related to the general

E–W extension of the Oligocene West European Rift (Bergerat, 1985).

Finally, the last major phase that can be reliably reconstructed is the strike-slip type compression, with a  $\sigma_1$  axis trending approximately 070° (Fig. 8). This can be interpreted as an early Miocene episode of the Alpine compression.

### **Conclusions**

The qualitative and quantitative tectonic analyses of brittle structures, at macroscopic and microscopic scales, enables us to understand the distribution and the evolution of the paleostress field near the Sainte-Victoire Range and the surrounding areas, and to provide an explanatory model for the regional-scale structures. Near the Sainte-Victoire Range, by contrast with the Arc basin (Gaviglio and Gonzales, 1987), geometrical interactions between folding and faulting, and syntectonic sedimentary formations are present. These characteristics allowed us to recognize the main steps of the tectonic evolution and to establish a second-order succession of stress regimes during the N–S compression, from the late Cretaceous to the late Eocene.

Concerning the methodology, a complex succession of tectonic events, involving common directions of compression, could be reliably deciphered. This study provides further evidence for the present interest in combining analyses of independent paleostress indicators, in accurate paleostress reconstructions.

### **Acknowledgements**

This work was supported by the Institut Français du Pétrole, represented by J. Letouzey. The authors thank C. Tourneret for providing computer programs, and the anonymous reviewers and the Editor-in-Chief M. Friedman for their constructive comments, which resulted in major improvements to the paper.

### **References**

- Angelier, J., 1984. Tectonic analysis of fault slip data sets. *J. Geophys. Res.*, 89 (B7): 5835–5848.

- Angelier, J., Tarantola, A., Valette, B. and Manoussis, S., 1982. Inversion of field data in fault tectonics to obtain the regional stress. I. Single phase fault populations: a new method of computing the stress tensor. *Geophys. J. R. Astron. Soc.*, 69: 607–621.
- Arthaud, F. and Choukroune, P., 1972. Méthode d'analyse de la tectonique cassante à l'aide des microstructures dans les zones peu déformées. Exemple de la plate-forme Nord-Aquitaine. *Rev. Inst. Fr. Pét.*, 27 (5): 715–732.
- Barquins, M., Ghalayini, K. and Petit, J.P., 1989a. Branchement des fissures sous compression uniaxiale. *C. R. Acad. Sci., Paris*, 308, II: 899–905.
- Barquins, M., Ghalayini, K., Maugis, D. and Petit, J.P., 1989b. Cinétique de propagation des fissures branchées sous compression uniaxiale. *C. R. Acad. Sci., Paris*, 309, II: 1451–1456.
- Bergerat, F., 1985. Déformations cassantes et champs de contrainte tertiaires de la plate-forme carbonatée européenne. Thèse de Doctorat-es-Sciences, Mém. Sci. Terre Univ. P. et M. Curie, no. 85-07, Paris, 315 pp.
- Bott, M.H.P., 1959. The mechanism of oblique slip faulting. *Geol. Mag.*, 96, 2: 109–117.
- Carey, E. and Brunier, B., 1974. Analyse théorique et numérique d'un modèle mécanique élémentaire appliqué à l'étude d'une population de failles. *C. R. Acad. Sci., Paris*, (D), 279: 891–894.
- Catzigras, F., Coulomb, E., Durand, J.P., Guieu, G., Rousset, C., Tempier, C., Nury, D. and Rouire, J., 1969. Geological map Aix en Provence, 1/50, 000e. B.R.G.M., Orleans, France.
- Corroy, G., Durand, J.P. and Tempier, C.I., 1964. Evolution tectonique de la montagne Sainte-Victoire. *Bull. Soc. Géol. Fr.*, VI: 91–106.
- Dietrich, D. and Song, H., 1984. Calcite fabrics in a natural shear environment, the Helvetic nappes of western Switzerland. *J. Struct. Geol.*, 6: 19–32.
- Durand, J.P. and Tempier, C., 1962. Etude tectonique de la zone des brèches du massif de Sainte Victoire dans la région du Tholonet (Bouches du Rhône). *Bull. Soc. Géol. Fr.*, IV: 97–101.
- Etchecopar, A., 1984. Etude des états de contraintes en tectonique cassante et simulation de déformations plastiques (approche mathématique). Unpublished Thèse de Doctorat-es-Sciences, Univ. Sciences et Techniques du Languedoc, Montpellier, 170 pp.
- Etchecopar, A., Vasseur, G. and Daignieres, M., 1981. An inverse problem in microtectonics for the determination of stress tensor from fault striation analysis. *J. Struct. Geol.*, 3: 51–65.
- Friedman, M. and Conger, F.B., 1964. Dynamic interpretation of calcite twin lamellae in a naturally deformed fossil. *J. Geol.*, 72: 361–368.
- Friedman, M. and Heard, H.C., 1974. Principal stress ratios in Cretaceous limestones from Texas Gulf coast. *Am. Assoc. Pet. Geol. Bull.*, 58(1): 71–78.
- Friedman, M. and Stearns, D.W., 1971. Relations between stresses derived from calcite twin lamellae and macrofractures, Teton anticline, Montana. *Geol. Soc. Am. Bull.*, 82: 3151–3162.
- Gaviglio, P. and Gonzales, J.F., 1987. Fracturation et histoire tectonique du bassin de Gardanne (Bouches du Rhône). *Bull. Soc. Géol. Fr.*, III, 4: 675–682.
- Gonzales, J.F., 1989. La déformation cassante dans le bassin de Gardanne (Provence). Aspect microtectonique de l'influence structurale du Régagnas. Unpublished Thèse de Doctorat-es-Sciences, Univ. Provence, Aix-Marseille, 164 pp.
- Lacombe, O., Angelier, J., Bergerat, F. and Laurent, Ph., 1990a. Tectoniques superposées et perturbations de contrainte dans la zone transformante Rhin-Saône: apport de l'analyse des failles et des macles de la calcite. *Bull. Soc. Géol. Fr.*, (8), VI, 5: 853–863.
- Lacombe, O., Angelier, J., Laurent, Ph., Bergerat, F. and Tourneret, Ch., 1990b. Joint analyses of calcite twins and fault slips as a key for deciphering polyphase tectonics: Burgundy as a case study. *Tectonophysics*, 182: 279–300.
- Larroque, J.M. and Laurent, Ph., 1988. Evolution of the stress field pattern in the south of the Rhine graben from the Eocene to the present. *Tectonophysics*, 148: 41–58.
- Laurent, Ph., 1984. Les macles de la calcite en tectonique: nouvelles méthodes dynamiques et premières applications. Unpublished Thèse de Doctorat-es-Sciences, Univ. Sciences et Techniques du Languedoc, Montpellier, 324 pp.
- Laurent, Ph., Bernard, Ph., Vasseur, G. and Etchecopar, A., 1981. Stress tensor determination from the study of *c* twins in calcite: a linear programming method. *Tectonophysics*, 78: 651–660.
- Laurent, Ph., Tourneret, Ch. and Laborde, O., 1990. Determining deviatoric stress tensors from calcite twins: application to monophased synthetic and natural polycrystals. *Tectonics*, 9 (3): 379–389.
- Letouzey, J., 1986. Cenozoic paleo-stress pattern in the Alpine foreland and structural interpretation in a platform basin. *Tectonophysics*, 132: 215–231.
- Mattauer, M. and Mercier, J.L., 1980. Microtectonique et grande tectonique. *Mem. Soc. Géol. Fr., Hors Sér.*, 10: 141–161.
- Nury, D., 1980. Tectoniques superposées dans la série oligocène de Marseille (Bouches du Rhône). *Bull. BRGM*, 2 (I), 1: 69–74.
- Petit, J.P. and Barquins, M., 1990. Fault propagation in mode II conditions: comparison between experimental and mathematical models, applications to natural features. *International Conferences on Mechanics of Jointed and Faulted Rocks*, Vienna, Austria, 18–20 April 1990. *Rossmamith*, pp. 213–220.
- Rowe, K.J. and Rutter, E.H., 1990. Paleo-stress estimation using calcite twinning: experimental calibration and application to nature. *J. Struct. Geol.*, 12, 1: 1–17.
- Taha, M., 1986. Apport de la microtectonique au problème des trajectoires de contraintes et de leurs perturbations (exemple du Nord de Montpellier). Unpublished Thèse de

- Doctorat-es-sciences, Univ. Sciences et Techniques du Languedoc, Montpellier, 155 pp.
- Tempier, C., 1987. Modèle nouveau de mise en place des structures provençales. *Bull. Soc. Géol. Fr.*, 8 (3): 533–540.
- Tempier, C. and Durand, J.P., 1981. Importance de l'épisode tectonique d'âge Crétacé supérieur dans la structure du versant méridional de la montagne Sainte-Victoire (Provence). *C. R. Acad. Sci., Paris*, 293: 629–632.
- Tourneret, Ch. and Laurent, Ph., 1990. Paleostress orientations from calcite twins in the north pyrenean foreland, determined by the Etchecopar inverse method. *Tectonophysics*, 180: 287–302.
- Trémolières, P., 1981. Mécanismes de la déformation en zones de plate-forme: méthode et application au bassin de Paris. *Rev. Inst. Fr. Pét.*, 36 (4): 395–428 and 579–593.
- Tullis, T.E., 1980. The use of mechanical twinning in minerals as a measure of shear stress magnitudes. *J. Geophys. Res.*, 85: 6263–6268.
- Turner, F.J., 1953. Nature and dynamic interpretation of deformation lamellae in calcite of three marbles. *Am. J. Sci.*, 251: 276–298.
- Turner, F.J., Griggs, D.T. and Heard, H., 1954. Experimental deformation of calcite crystals. *Geol. Soc. Am. Bull.*, 65: 883–934.
- Xiaohan, L., 1983. (I) Perturbations de contraintes liées aux structures cassantes dans les calcaires fins du Languedoc: observations et simulations mathématiques. (II) Mesure de la déformation finie à l'aide de la méthode Fry: application aux gneiss des Bormes (massif des Maures). Unpublished Thèse de Doctorat-es-Sciences, Univ. Sciences et Techniques du Languedoc, Montpellier, 152 pp.